

# Scalable Video Transmission over the IEEE 802.11e Networks Using Cross-Layer Rate Control

Chuan Heng Foh, Yu Zhang, Zefeng Ni, Jianfei Cai  
Centre for Multimedia and Network Technology  
School of Computer Engineering  
Nanyang Technological University  
Singapore

**Abstract**—This paper presents a novel cross-layer rate control scheme for optimizing 3D wavelet scalable video transmission over the IEEE 802.11e wireless local area networks. The proposed scheme consists of a macro and a micro rate control schemes residing at the application layer and the network sublayer respectively. The macro rate control uses bandwidth estimation to achieve optimal bit allocation with minimum distortion. The micro rate control employs an adaptive mapping of packets using video classifications. This prioritizes appropriately the video traffic to maximize the transmission protection to the important video packets. The performance is investigated by simulations showing advantages of our cross-layer design.

## I. INTRODUCTION

Given the growing popularity of real-time services and multimedia based applications, it has recently become more critical to tailor IEEE 802.11 medium access control (MAC) protocol to meet the stringent requirements of such services. The IEEE 802.11 working group has developed a new standard known as the IEEE 802.11e [1] to provide the quality of service (QoS) support. The IEEE 802.11e defines a single coordination function, called the hybrid coordination function (HCF), which includes two medium access mechanisms: contention-based channel access and controlled channel access. In particular, the contention-based channel access is referred to as enhanced distributed channel access (EDCA), which extends the legacy distributed coordination function (DCF) [2] by providing the MAC layer with per-class service differentiation.

Among various applications, video streaming is one of the most attractive applications for WLANs. In order to be adaptive to time-varying wireless network conditions and diverse scenarios, video adaption is indispensable. Scalable video coding (SVC) [3] is the latest video coding technique, which provides great flexibility in video adaptation since it only needs to encode a video once and the resulted bitstream can be decoded at multiple reduced rates and resolutions. Recently, we have seen extensive studies such as [4], [5] on streaming scalable video over lossy networks. The common idea is to use unequal error/loss protection (UEP/ULP), i.e. giving the more important information more protection, to explore the fine granularity scalability provided by SVC. Such an ULP idea has been implemented differently in different network layers. However, most of the existing ULP approaches only

consider a single end-to-end connection and focus on optimally distributing network resource among different priorities under the constraint of a fixed total network resource. From the entire network point of view, the resource distribution in one connection might not be independent of other competing connections. Thus, the ULP strategy for one user should aim at not only maximizing its own video quality but also minimizing the harmful effect to other users.

In this paper, we propose a practical cross-layer design for transmitting scalable video over WLANs. In particular, we propose a *macro* and a *micro* rate control schemes at the application layer and the network sublayer respectively. At the application layer, the macro rate control minimizes the distortion of the video quality given the bandwidth constraint by optimal bit allocation in our developed SVC. At the network sublayer, the micro rate control performs further rate cut by packet drops when network experiences congestion before the application can react with the macro rate control. Through an adaptive QoS mapping, the micro rate control enforces ULP that drops video packet with low importance to protect the transmission of those with high importance. This combination ensures optimization of video streaming over the IEEE 802.11e WLAN.

The rest of the paper is organized as follows. Section II describes our proposed cross-layer design in detail. Section III gives the experiment results highlighting the benefits of our proposed design. Finally, Section IV concludes this paper.

## II. CROSS-LAYER DESIGN

In order to enable the easy adaptation of wireless video streaming, we develop a simple scalable video coding scheme based on the integration of the motion compensated temporal filtering (MCTF) [6] and JPEG2000. In particular, each color component (YUV) of the original frames is first filtered using MCTF with 5/3 wavelet. MCTF is applied iteratively to the set of low-pass bands in order to provide multiple frame rates in the final scalable bitstream. Through MCTF, we generate the motion vectors and many temporal bands (T-bands). Each T-band can be treated as an individual image. Then, JPEG2000 is used to encode these T-bands into multiple quality layers, each of which has a R-D value. After removing those non-feasible truncation points, optimal bit truncation is performed to reach the given targeted bitrate. The final video bitstream

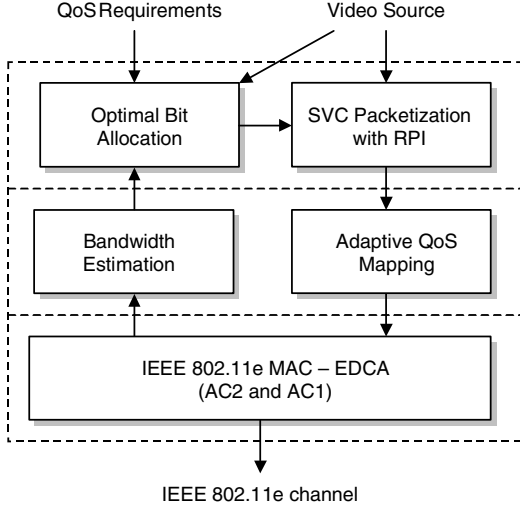


Fig. 1. Block diagram of the proposed cross-layer QoS design.

consists of the MV information generated by MCTF and the JPEG2000 bitstream for each T-band.

Our proposed cross-layer design is presented in Fig. 1. The design uses rate control to optimize quality performance for transmitting the scalable video over IEEE 802.11e EDCA. The application layer and network sublayer cooperate to decide the optimal transmission strategy for the scalable video stream. The common knowledge of the two layers is the available bandwidth which is the main factor dictating the employed transmission strategy at each layer. In brief, based on the detected network available bandwidth at the network sublayer, the application layer decides the encoding strategy and produces video streams that fit into the available bandwidth with the best possible video quality. However, the slower timescales at the application layer makes it difficult to respond to rapid bandwidth variation. To cope with this bandwidth variation at a smaller timescale, especially a sudden downside change in the available bandwidth, using the traffic information passed down from the application layer, the network sublayer reacts with a further transmission rate adjustment subjected to minimum distortion. This design of rate controls, where the application layer and the network sublayer perform *macro* and *micro* rate controls respectively, provides all timescale rate adaptation for video delivery over EDCA. As shown in Figure 1, the macro rate control is achieved by the coordination between the bandwidth estimation and optimal bit allocation components while the micro rate control is achieved by the coordination between the SVC packetization with relative priority index (RPI) and adaptive QoS mapping components.

#### A. Optimal Bit Allocation in SVC

The problem of optimal bit truncation can be summarized as: *given the estimated bandwidth  $R$  from the network sublayer, how to optimally truncate each T-band JPEG2000 stream so that the overall distortion can be minimized?* For our developed fully scalable video coding, there are many ways to allocate bits among T-bands by making trade off among

frame rates, spatial resolution and SNR of individual frames. However, an optimal tradeoff among the three scalabilities is still an open question. In this paper, for simplicity, we only consider using the SNR scalability to match the estimated network bandwidth. In particular, considering each T-band JPEG2000 stream contains a number of quality layers whose corresponding rates and distortions are known, we directly use these quality layers of JPEG2000 streams as the available truncation points although JPEG2000 provides even finer truncation points. The bit allocation algorithm is similar to the optimal truncation in JPEG2000 [7].

#### B. SVC Packetization with Relative Priority Index

For the packetized video transmission, T-band streams and MV data need to be assembled into individual network packets. In this paper, we simply put different color component into different packets and place motion vectors into the first packet of their associated temporal high bands. The size of a packet is limited by a predefined maximum packet size  $P_{size}$ .

In order to provide adaptive QoS mapping in the network sublayer, it requires the application layer to provide the relative priorities of video packets. In this research, we apply the concept of RPI proposed in [5] to categorize different video packets. In particular, we use the loss impact of a packet to calculate its RPI. The loss impact of a packet is defined as the corresponding distortion increase in reconstructed video in the case that the packet is lost while all other packets are correctly received. Mathematically, the loss impact of the  $i$ -th packet in the T-band  $B$  of the color component  $C$  is calculated as

$$W_C \times G_B \times (D_{i-1,B,C} - D_{i,B,C}), \quad (1)$$

where  $D_{i,B,C}$  is the distortion up to the  $i$ -th packet,  $G_B$  is the energy gain associated for the T-band  $B$  and  $W_C$  is the weight ( $W_C = 1$  by default) for each color component if we want to assign the YUV components with different priorities.

Moreover, in order to enable smooth adjustment of the QoS mapping in the network sublayer, we map the loss impact values obtained in (1) into integer RPI values (e.g. 0-63 with 8 bits representation), and also uniformly distribute the integer RPI values into different packets. The detailed procedure of generating RPI values is summarized as follows. First, we sort all the packets according to their calculated loss impact values in a decreasing order. Then, for each packet  $i$ , we identify its position  $Pos_i$  in the sorted list. Assuming the RPI values ranging from 0 to  $M - 1$ , we define that the packets with smaller RPI value are more important. For a total number of  $N$  packets, we calculate RPI as

$$RPI_i = \lfloor Pos_i / N \times (M - 1) \rfloor. \quad (2)$$

#### C. Bandwidth Estimation in EDCA

Bandwidth estimation is an important component in our cross-layer design. The application layer and network sublayer depend on this estimation to achieve rate control and optimize QoS. The main role of the bandwidth estimation is to measure the network condition during a macro interval and provide

estimation of available capacity that a node can access in the next macro interval.

Our design adopts IdleGap [8] to estimate the network bandwidth availability. However, the estimated available bandwidth will be shared among all nodes, thus the bandwidth accessible by each node is usually lower. To ensure that each node only utilizes its share of the available bandwidth, we introduce a simple method described as follows. We first notice that multimedia transmissions usually occurs in a form of continuous streams. The detection of a video packet from a node indicates the participation of multimedia transmissions. Hence we propose that during a macro interval, not only a node estimates the network available bandwidth,  $\tilde{R}$ , using IdleGap, it also detects and counts the number of different nodes,  $\tilde{N}$ , that transmit packets. Using the two quantities, also including itself as a transmitting source,  $\tilde{R}/(\tilde{N} + 1)$  represents the estimated available bandwidth for a node in the next interval. If a node also transmitted  $\tilde{T}$  video traffic during the current macro interval, then by the end of the current interval, the node estimates its available bandwidth,  $R$ , for the next interval simply by  $R = \tilde{T} + \frac{\tilde{R}}{\tilde{N}+1}$ .

#### D. Adaptive QoS Mapping

Scalable video traffic consists of packets carrying video information of different important relative priority index. These packet transmissions must receive different error and loss protection to exploit the scalable video benefit. Using the characteristics of the EDCA queues, we design a stream mapping strategy that adaptively maps packets of scalable video traffic onto two EDCA Access Categories (ACs) with ULP. We choose AC2 as one of the queue since its default purpose is to carry video traffic. AC1, which is used for best effort according to the IEEE 802.11e standard, is another chosen queue. It is used here to carry less important scalable video traffic. Packets mapped onto AC1 are prepared to make sacrifices in forms of packet drops under heavy network load conditions. These sacrifices make room for more important video packets to be transmitted successfully, and hence achieving higher QoS of video transmissions.

Table I presents our proposed QoS mapping algorithm. The algorithm consists of an adaptive QoS mapping mechanism to map prioritized video traffic onto two EDCA queues with ULP. The QoS mapping design takes into the consideration of the EDCA characteristics that two ACs of EDCA utilize different throughput on the channel. To understand the EDCA queue characteristics for the QoS mapping algorithm design, we analytically evaluate the IEEE 802.11e EDCA performance related to ULP.

We extend our earlier developed Markov Chain model [9] for our study. Details of the extended model are presented in Appendix I. We consider the IEEE 802.11e system parameters listed in Table II where  $CW_{min}$ ,  $CW_{max}$ , and AIFSN are Minimum Contention Window, Maximum Contention Window, and Arbitration Interframe Space Number, respectively. These constants follow the latest standard [1] whenever specified, otherwise, typical values applied. Our model takes  $n_i$  and  $u_i$  as inputs and gives throughput and packet loss probability

TABLE I  
DESCRIPTION OF ADAPTIVE QoS MAPPING ALGORITHM

---

Let  $SRPI$  denote the set of RPI values.  
 Let  $\hat{v}_i$  denote the remaining traffic volume of each RPI (in bits).  
 Let  $\Lambda$  denote the mapping pointer where packets with  $RPI \leq \Lambda$  is inserted to AC2 queue, otherwise, they are inserted to A1 queue.

```

procedure ComputePointer( $\hat{v}_i$ )
   $\hat{v} := \sum_i \hat{v}_i$ 
  return  $\max(i)$  such that  $\sum_i \hat{v}_i \leq \frac{2}{3} \hat{v}$ 
end

procedure PacketDepartureEvent( $i, s$ )
  // Packets departing the network may be due to either a
  // successful transmission or a loss.
  //  $i$  is the RPI of the departing packet.
  //  $s$  is the size (in bits) of the departing packet.
   $\hat{v}_i := \hat{v}_i - s$ 
   $\Lambda = \text{ComputePointer}(\hat{v}_i)$ 
end

procedure StartMacroIntervalEvent( $c$ )
  //  $c$  is a vector containing the expected traffic volume
  // of each RPI during a macro interval.
  for each  $i$  in  $SRPI$  do
     $\hat{v}_i := c_i$ 
  end for
   $\Lambda = \text{ComputePointer}(\hat{v}_i)$ 
end

```

---

as outputs, where  $u_i$  describes video traffic offered load of a node given a total of  $n_i$  statistically identical nodes in AC $i$ ,  $i = 1, 2$ .

TABLE II  
IEEE 802.11e MAC PROTOCOL SYSTEM PARAMETERS

Access category	AIFSN	$CW_{min}$	$CW_{max}$	Queue length	Maximum retry limit, $r$
AC3	2	7	15	25	8
AC2	2	15	31	25	8
AC1	3	31	1023	25	4
AC0	7	31	1023	25	4

Based on our model, we first evaluate the service rates differentiation of the standardized IEEE 802.11e EDCA mechanism. The service rates in different EDCA queues are mainly dictated by their contention window sizes and AIFSN settings. To analyze the service rate differentiation between AC2 and AC1, we compare the saturation throughput between AC2 and AC1 under various network load conditions. The saturation load condition is considered because it stresses the queue utilization and the channel usage, and threatens packet loss, which is of our main interest of study. The number of saturated nodes directly dictates the load of the network. Varying the number of saturated nodes gives a range of network load conditions. The network load condition can also be indicated by the collision probability, where with a low (high) number of saturated nodes, the collision probability that a packet suffers is low (high) indicating light (heavy) network load. Fig. 2 plots the service ratio of the throughput of AC2 to that of AC1 versus the collision probability of AC2. The collision probability of AC2 is a more accurate measure in this study because it counts only the external collision probability whereas that of AC1 includes also the internal collision which

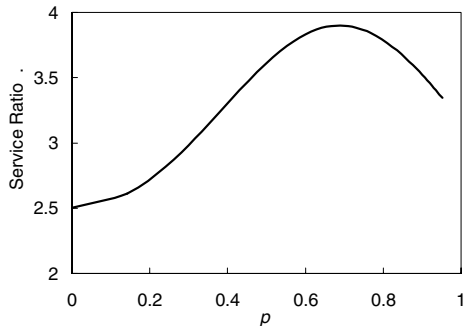


Fig. 2. The ratio of the throughput of AC2 to that of AC1 in an EDCA node under various network load conditions.

is termed the virtual collision in the IEEE 802.11e standard.

As shown in Fig. 2, the service ratio ranges from two to four under various load conditions. This means that AC2 is capable of transmitting two to four times faster than AC1 thus achieving service differentiation. This result provides a guideline for the design of mapping from the priority of scalable video traffic to the priority of the two considered EDCA queues. To optimize the queue usage in the system, it is necessary that packets in both queues be built or cleared up at a similar rate. Since our result as presented in Fig. 2 suggests that AC2 is capable to transmit more packets than AC1 in a given time interval, it is expected that more packets should be queued in AC2 than in AC1. Moreover, based on the EDCA queue metrics, AC2 and AC1 should serve high and low prioritized packets of the scalable video traffic respectively.

However, maintaining the same utilization in the queues of AC2 and AC1 provides unbiased loss protection to the two queues since both queues are equally likely to drop packets under heavy load condition. To facilitate ULP in EDCA for the scalable video traffic, our mapping design considers a lower ratio of throughput of AC2 to that of AC1 than the service ratios presented in Fig. 2. Theoretically, any value below the presented curve may be adopted yielding different levels of inequality in loss protection. In order not to differ too far from the theoretical results so as to maintain certain optimality in queue utilization, we choose the service ratio two as our mapping strategy. In other words, with our design (see also Table I), AC2 is responsible for the top 2/3 scalable video traffic in terms of the priority, while AC1 is responsible for the remaining bottom 1/3 traffic. Since our mapping inserts lesser traffic to AC2 than the suggested optimum value, packet built-up rate in AC2 is slower, and hence packets queued in AC2 receive higher protection from overflow at the expense of the lower protection to AC1. It is thus expected that under heavy load conditions, overflow is likely to occur in AC1 before AC2. However, occurrence of overflow in AC2 is inevitable if the service ratio of the mapping remains unchanged. To tackle this problem, we further introduce an adaptiveness into our mapping design to reduce the chances of overflow in AC2.

To further strengthen the ULP in EDCA, we follow the design in [10] that different maximum retry limit settings are applied to different EDCA queues as shown in Table II.

In the macro control, the application controls the source

rate based on the bandwidth estimated from the network sublayer within an interval. With the advantage of knowing the total volume of generated traffic from the application within a macro interval, our adaptive QoS mapping attempts to maintain a two to one service ratio of AC2 to AC1 for the mapping based on the remaining traffic volume rather than the fixed total traffic volume. The mapping point hence floats and changes based on the situation of the network condition.

### III. EXPERIMENTAL RESULTS

In this section, we present the performance of the 3D wavelet SVC over the IEEE 802.11e WLANs. In our experiments, we consider the first 256 frames of the “Table-tennis” CIF sequence as our video source. The sequence is repeatedly transmitted for simulation time requirement. Two levels of MCTF decomposition is used during encoding of the video. The maximum video packet size is set to 500 bytes. The RPI ranges between 0 and 63. The macro interval is set to 32/30 seconds. We take the Y component PSNR as our video quality measurement.

The experiments are conducted using ns2 [11]. The IEEE 802.11e settings follow the latest standard presented in Table II. The performance is also compared with DCF and EDCA. The former refers to the legacy DCF with setting following the IEEE 802.11b standard [2], and the latter refers to the EDCA using AC2 for video transmission with no cross-layer consideration. Our considered network is a single hop private infrastructure WLAN. This setup allows us to focus solely on the WLAN.

Each experiment starts with one node, labeled as node-0, transmitting a certain rate of video traffic. For every four macro interval duration, a new video node is added to the WLAN, until the number of nodes reaches 15 in the WLAN.

Figures 3-4 plots the PSNR performance measured at node-0 under DCF and EDCA respectively. Two fixed source rates, which are 500 kbps and 1 Mbps, are used. As can be seen, DCF supports merely three (seven) nodes for the case of 1 Mbps (500 kbps) of video source rate before the PSNR plunges quickly due to network congestion. A simple calculation reveals that the maximum achievable network throughput is no more than 4 Mbps. Similar observation is made for EDCA as indicated in Fig. 4. The results also show the maximum achievable network throughput of no more than 4 Mbps. This result reveals that when source rate is left uncontrolled, the network may be pushed to saturation where the protocol operates at a lower throughput level.

For our scheme, since the macro rate control is in place, each node varies its source rate according to the estimated available bandwidth from no less than 500 kbps to no more than 1 Mbps. A node always starts from the maximum specified rate of 1 Mbps. The performance result is presented in Fig. 5. An immediate comparison among Figs. 3-4 shows the performance advantage of our cross-layer design. The soft capacity property of our scheme is also clearly illustrated. As can be seen from Fig. 5, when the network consists of a small number of nodes, each node receives high quality video streams. As the simulation progresses, the number of

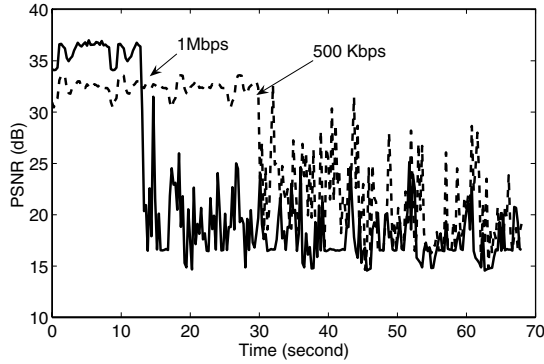


Fig. 3. PSNR of received video for DCF.

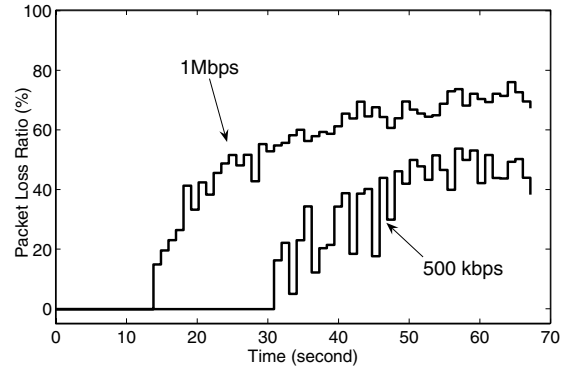


Fig. 6. Packet loss ratio for DCF.

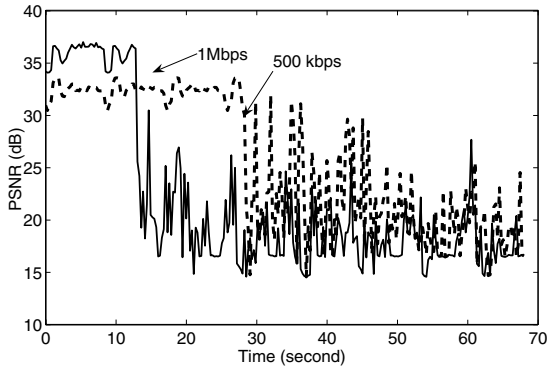


Fig. 4. PSNR of received video for EDCA.

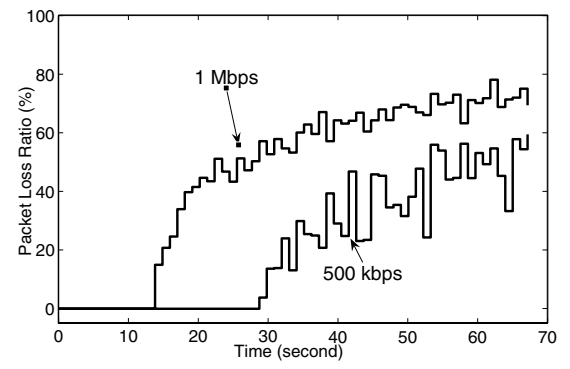


Fig. 7. Packet loss ratio for EDCA.

nodes increases, all nodes adapt themselves to the changed network condition to accommodate more nodes by reducing the sending rate. Even though we specify our minimum macro rate to 500 kbps, the micro rate control drops video packets of low importance via AC1 so that the quality of the video streams maintained even at as many as 15 nodes.

To further illustrate the performance advantages of our scheme, we compare the packet loss ratio (in percentage) in Figs. 6-8. As shown in the figures, DCF and EDCA share the similar behavior in terms of packet loss ratio. With no cross-layer consideration, important video packets may be dropped and hence quality of video streams cannot be maintained when packet loss occurs. On the other hand, the ULP in our adaptive

QoS mapping protects video packets on AC2 by sacrificing packets on AC1. There is hardly any loss experienced at AC2.

#### IV. CONCLUSION

In this paper, we have presented the cross-layer design that achieves all timescales rate control for optimizing 3D wavelet scalable video transmission over the recently standardized IEEE 802.11e networks. We performed the analysis of EDCA and study the characteristics of EDCA for our cross-layer design. We further carried out computer simulation to investigate the performance of our proposed design. Experimental results have shown that our scheme outperforms all other considered

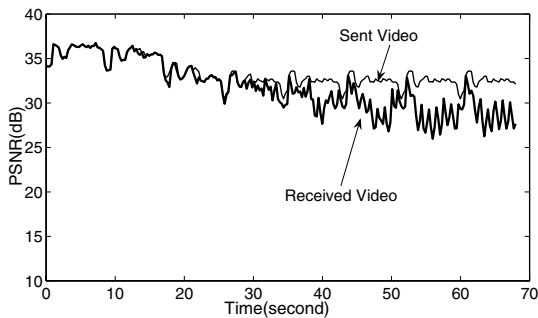


Fig. 5. PSNR for our cross-layer design.

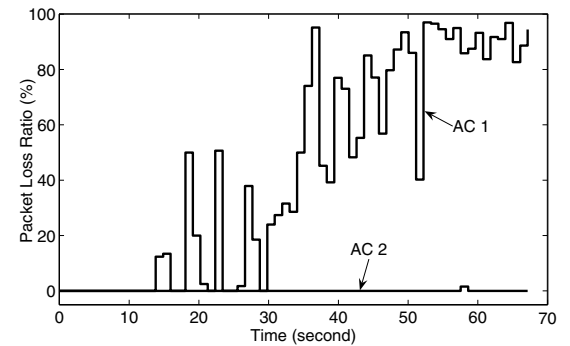


Fig. 8. Packet loss ratio for our cross-layer design.

methods including DCF and the standardized EDCA with no cross-layer consideration.

## APPENDIX I

This section presents the EDCA analytical study for the justification of our QoS mapping design. According to our previous study in [9], due to the different AIFSN values standardized for AC2 and AC1, two Markov Chains are developed, referred as *Chain A* and *Chain B*, to model the backoff procedure of AC2 and AC1 respectively. The following list defines the variables in a particular chain associated with a certain AC. Details are also given in [9].

$W_{j,i}$  : The backoff window size at stage  $j$  of  $AC_i$ , where  $W_j = 2^{\min(j,m)}(CW_{min} + 1)$  and  $CW_{min}$  of the associated AC is specified in the IEEE 802.11e standard (see also Table II).

$m_i$  : The maximum backoff stage of  $AC_i$ . That is,  $W_m = CW_{max} + 1$  where  $CW_{max}$  of the associated AC is specified in the IEEE 802.11e standard (see also Table II).

$r_i$  : The maximum retry limit of  $AC_i$ . We follow the value specified in [10] (see also Table II).

$u_i$  : The probability that after a successful transmission by a node using  $AC_i$ , its queue remains empty after either an idle or a busy slot duration.

$p_i$  : The probability that a transmission of  $AC_i$  suffers a collision.

$q_1$  : The probability that a transmission does not occur in a slot given that the previous slot is busy. This variable only applies to *Chain B*.

$q_2$  : The probability that a transmission does not occur in a slot given that the previous slot is idle. This variable only applies to *Chain B*.

We reuse the analytical approach and extend the model to include unsaturation traffic consideration. An extra state  $\{0, -1\}$  ( $\{0, -1, 0\}$ ) with given a recurrent probability are added into *Chain A* (*Chain B*) to describe the idle period of a node. The recurrent probability,  $u_i$ , is the input of the system, which is used to control the offered load of each node. The new balance equations for the two chains are presented in the following.

Let  $\alpha_{i,j}(p, u)$  be the stationary distribution of *Chain A* given that the collision and unsaturation probabilities for the associated AC are  $p$  and  $u$  respectively. Owing to the chain regularities and imposing the stationary probability normalization, we have

$$\alpha_{0,0}(p, u) = \begin{cases} \left( \frac{\iota_r + \kappa}{\xi} + \frac{u}{1-u} \right)^{-1}, & r \leq m \\ \left( \frac{\iota_m + \kappa + \nu}{\xi} + \frac{u(1+(r-m)p^m(1-p))}{1-u} \right)^{-1}, & r > m \end{cases} \quad (3)$$

where  $\xi$ ,  $\iota$ ,  $\kappa$ , and  $\nu$  are given by

$$\begin{aligned} \xi &= 2(1-2p)(1-p) \\ \iota_r &= W_0(1-(2p)^{r+1})(1-p) \\ \iota_m &= W_0(1-(2p)^{m+1})(1-p) \\ \kappa &= (1-2p)(1-p^{r+1}) \\ \nu &= W_0 2^m p^{m+1}(1-2p)(1-p^{r-m}) \end{aligned} \quad (4)$$

Similarly for AC1, let  $\beta_{i,j,k}(p, u, q_1, q_2)$  be the stationary distribution of *chain B* given  $p$ ,  $u$ ,  $q_1$  and  $q_2$ , we obtain

$$\beta_{0,0,0}(p, u, q_1, q_2) = \begin{cases} \left( \frac{(1+q_1-q_2)\iota_r + (1+q_1+q_2)\kappa}{q_1\xi} + \frac{u}{1-u} \right)^{-1}, & r \leq m \\ \left( \frac{(1+q_1-q_2)(\iota_m + \nu) + (1+q_1+q_2)\kappa}{q_1\xi} + (1+(r-m)p^m(1-p))\frac{u}{1-u} \right)^{-1}, & r > m \end{cases} \quad (5)$$

where  $\xi$ ,  $\iota$ ,  $\kappa$ , and  $\nu$  are given by (4). As in [9], the access probabilities are

$$\tau_i = \begin{cases} \frac{(1-p_i^{r_i+1})\beta_{0,0,0}(p_i, u_i, q_1, q_2)}{(1-p_i)P_I}, & i = 1 \\ \frac{(1-p_i^{r_i+1})\alpha_{0,0}(p_i, u_i)}{1-p_i}, & i = 2 \end{cases} \quad (6)$$

where

$$\begin{aligned} P_I &= q_1 P_B + q_2 P_I = \frac{q_1}{1+q_1-q_2} \\ P_B &= 1 - P_I \end{aligned} \quad (7)$$

and  $q_1 = (1 - \tau_2)^{n_2}$ ,  $q_2 = \prod_{i=1}^2 (1 - \tau_i)^{n_i}$ .

Let the number of nodes accessing the network of  $AC_i$  be  $n_i$ ,  $i = 1, 2$ , the collision probability  $p_i$ , can be written as

$$p_i = \begin{cases} 1 - (1 - \tau_i)^{n_i-1} \prod_{x \neq i} (1 - \tau_x)^{n_x}, & i = 1 \\ (1 - \prod_{x \leq i, x \neq 0} (1 - \tau_x)^{n_x-1} \prod_{x > i} (1 - \tau_x)^{n_x}) P_B \\ + (1 - \prod_{x \leq i} (1 - \tau_x)^{n_x-1} \prod_{x > i} (1 - \tau_x)^{n_x}) P_I, & i = 2. \end{cases} \quad (8)$$

The above formulas form a set of non-linear equations that can be solved numerically. These quantities can be used to compute the throughput and packet loss rate using the common approach [9].

## REFERENCES

- [1] IEEE, "Wireless LAN Medium Access Control (MAC) and Physical Layer (PHY) specifications Amendment 8: Medium Access Control (MAC) Quality of Service Enhancements," IEEE Std 802.11e-2005, IEEE, New York, 2005.
- [2] IEEE, "IEEE Standard for Information Technology - Telecommunications and Information Exchange between Systems - Specific Requirements Part 11: Wireless LAN MAC and PHY Specifications," IEEE Std 802.11-1999, IEEE, New York, 1999.
- [3] J.-R. Ohm, "Advances in scalable video coding," in *Proceedings of the IEEE*, vol. 93, pp. 4256, Jan. 2005.
- [4] P. A. Chou and Z. Miao, "Rate-distortion optimized streaming of packetized media," *Microsoft Research Technical Report*, Feb. 2001.
- [5] J. Shin, J. W. Kim, and C. C. J. Kuo, "Quality-of-service mapping mechanism for packet video in differentiated services network," *IEEE Trans. Multimedia*, no. 2, Jun. 2001.
- [6] A. Secker and D. Taubman, "Motion-compensated highly scalable video compression using an adaptive 3D wavelet transform based on lifting," in *Proc. IEEE Int. Conf. Image Processing*, vol. 2, 2001.
- [7] D. Taubman, "High performance scalable image compression with EBCOT," in *Proc. IEEE Int. Conf. Image Processing*, vol. 9, July 2000.
- [8] H. K. Lee, V. Hall, K. H. Yum, K. I. Kim, and E. J. Kim, "Bandwidth Estimation in Wireless LANs for Multimedia Streaming Services," *Proc. IEEE International Conference on Multimedia and Expo*, 2006.
- [9] J. W. Tantra, C. H. Foh, and A. B. Mnaouer, "Throughput and Delay Analysis of the IEEE 802.11e EDCA Saturation," *Proc IEEE International Conference on Communications*, 2005.
- [10] A. Ksentini, M. Naimi, and A. Gueroui, "Toward an Improvement of H.264 Video Transmission over IEEE 802.11e through a Cross-Layer Architecture," *IEEE Communications Magazine*, pp. 107-114, Jan. 2006.
- [11] <http://www.isi.edu/nsnam/>